4

DATA COLLECTION AND PROCESSING

4.1 INTRODUCTION

This chapter describes the hardware necessary for detecting and measuring traffic loads on bridges and the software developed by the author to process these measurements. Further details on the PC-based instrumentation used by the Irish team can be found in Appendix C. A B-WIM system is generally composed of devices to measure bridge strain, sensors to detect vehicle axles, a personal computer, software, signal conditioning and data acquisition (DAQ) hardware (Figure 3.1).

The bridge bending is measured either by strain gauges or reusable strain transducers. These devices produce an electrical signal proportional to the strain they are monitoring. If a B-WIM algorithm based on one sensor location is to be applied, this single longitudinal position is normally located in a main structural member at a point where strains get highest values (i.e. midspan in a simply supported beam). Multiple-sensor B-WIM algorithms use several longitudinal locations for more accurate weighing and their ideal number and location will be considered in Chapter 7.

Most existing B-WIM systems obtain the vehicle silhouette and velocity from axle detectors installed on the road surface. These detectors can be removable (tape switches, pneumatic tubes) or permanent (low-grade piezo-electric sensors or other built-in pavement sensors). Information on times is generated when an axle passes over them. If a pair of sensors is placed in each lane, it is possible to derive velocity and axle spacings for all vehicles. These axle detectors become unnecessary when a FAD (**F**ree **A**xle **D**etector) system is able to achieve the required accuracy. FAD identifies axles purely by measuring strain in appropriate locations of the bridge structure.

Software is composed of two main parts: Data acquisition and calculation of axle weights. Data acquisition is common to all B-WIM systems. This part of the program acquires

information on voltages from strain gauges/transducers and road sensors, while the latter part implements the B-WIM algorithm that converts voltages into weights. Three different approaches are described: CULWAY, SiWIM and the Irish DuWIM.

4.2 STRAIN MEASUREMENT

Strain (e) is defined as the fractional change in length shown in Figure 4.1.

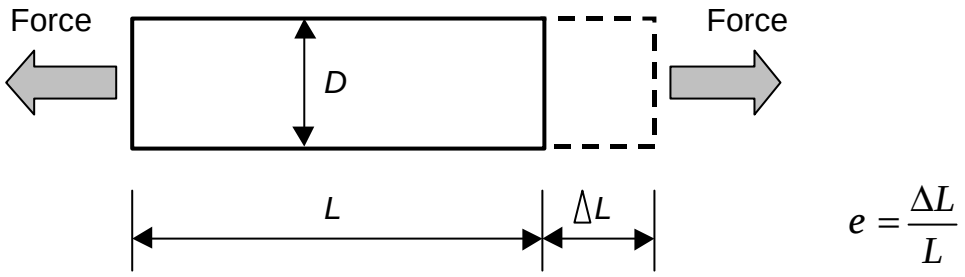

Figure 4.1 – Definition of strain (e)

Strain can be positive (tensile) or negative (compressive). The magnitude of measured strain is often expressed as microstrain ($1\ me = 10^{-6}\ e$).

Figure 4.2(a) shows a strain transducer and Figure 4.2(b) strain gauges glued directly onto the bridge deck. Several methods of measuring strain in bridges are presented next.

4.2.1 Strain gauges

The strain gauge is bonded to the bridge surface (Figure 4.2(b)). Then, the strain experienced by the bridge is transferred directly to the gauge, which responds with a linear change in electrical resistance.

(a) Strain transducer (after Jacob et al. 2000)

(b) Installation of strain gauges

Figure 4.2 – Instrumentation to measure strain in a bridge deck

The bonded metallic strain gauge is the most widely used, which consists of a very fine wire or, more commonly, metallic foil arranged in a grid pattern (Figure 4.3(a)). The cross sectional area of the grid is minimised to reduce the effect of shear strain. Strain is detected by the change in electrical resistance of the gauge grid. Because these changes in resistance are very small, strain gauges are usually measured in a Wheatstone Bridge configuration as shown in Figure 4.3(b).

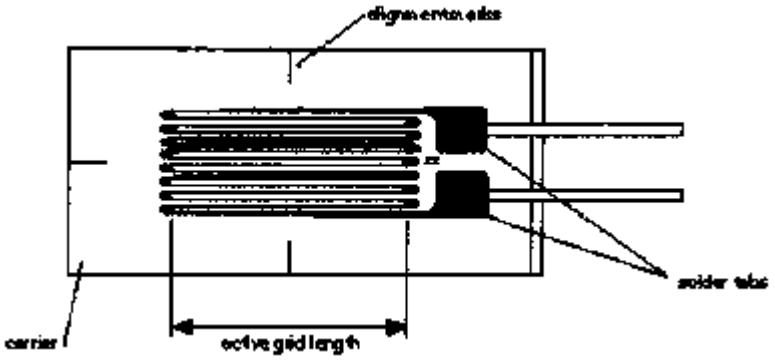

(a) Layout (b) Typical configuration

Figure 4.3 – Description of strain gauges

In this figure, R_1, R_2, R_3, and R_4 , represent resistors, and e_o and e_i the excitation voltage powering the Wheatstone bridge and the voltage measured by the DAQ system, respectively. The measured voltage, e_i, can be obtained by applying Ohm's laws, resulting in Equation 4.1. As strain is applied to the gauge, its resistance value changes, causing a change in the voltage at e_i.

$$e_i = \left(\frac{R_2}{R_2 + R_4} - \frac{R_1}{R_1 + R_3} \right) e_o \tag{4.1}$$

The Irish team has commonly been using strain gauges type PL-90[11]. This type is composed of polyester wire (Cu-Ni), with a normal operational temperature range from –20°C to 80°C and 120 Ω resistance. Strain is related to the fractional change in electrical resistance through the gauge factor (*GF*), a parameter that measures the sensitivity of the gauge. The gauge factor for metallic strain gauges is typically around 2.

Strain gauges can occupy one, two or four arms of the Wheatstone bridge, with any remaining positions filled with fixed resistors. One arm was used in the experiments in Belleville, France (Chapter 8), where the gauge was directly glued onto the steel bridge deck. In this case, R_4 was replaced with an active gauge subjected to the applied force, R_1 = R_3 are fixed resistors, and R_2 a dummy gauge with the same nominal value as R_4. By using an active and a dummy gauge, the effect of temperature is avoided. The temperature effects, identical for both gauges, do not change the ratio of their resistance or the measured voltage in Equation 4.1. Strain in this quarter bridge is given by Equation 4.2.

$$\varepsilon = \frac{-4\left(\frac{e_i(unstrained) - e_i(strained)}{e_o} \right)}{GF\left[1 + 2\left(\frac{e_i(unstrained) - e_i(strained)}{e_o} \right) \right]} \left(1 + \frac{R_L}{R_2} \right) \tag{4.2}$$

where R_L is the resistance in the lead wires of the strain gauges.

Alternatively, using two active gauges can double the sensitivity of the Wheatstone bridge. To achieve this, R_2 is mounted in compression and R_4 in tension, or vice versa. Using all four arms of the Bridge can further increase sensitivity. To achieve this, R_2 and R_3 are mounted in compression, and R_1 and R_4 are mounted in tension. Equation 4.2 changes when using such half or full Bridges. These two configurations are applied to the mechanical strain amplifier described in the following section.

4.2.2 Strain Amplifiers

Strain amplifiers are necessary when a better strain definition than the one occurring in the structure is required. The principle of a mechanical strain amplifier is concentrating the elongation or shortening of a given length on the bridge into a highly strained section of the amplifier. The mechanical strain amplifiers are connected to the deck of the bridge via either steel anchor plates that are glued or bolted to the bridge deck or by directly bolting the gauge to the structure.

Different models of strain amplifier are shown in Figure 4.4. There are two different approaches: a) Amplification by direct measurement of axial deformation into a smaller and more flexible inner section (Peters 1984, González 1996) and b) Amplification of strain by conversion of axial deformation into localised bending (Peters 1984, Dempsey 1997). The latter approach has been proven to be more robust and stable according to the Australian and Irish experience. The Irish model is reviewed next.

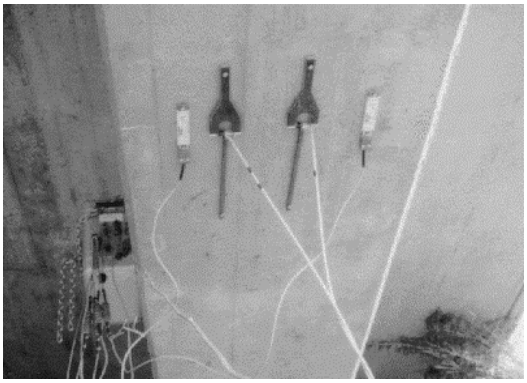

(a) Commercial strain transducers (outside) and Irish mechanical strain amplifiers (inside) attached to a bridge soffit (after Jacob et al. 2000)

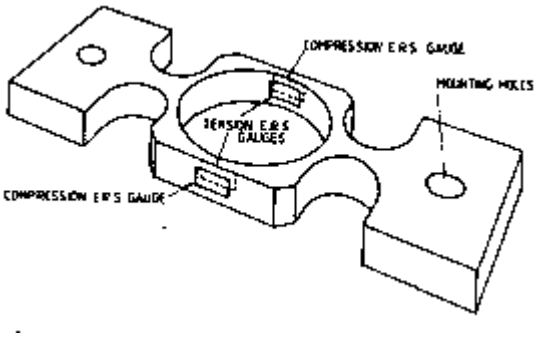

(b) Australian mechanical strain amplifier (after Peters 1984)

Figure 4.4 – Strain Transducers

Irish Model

This Irish amplifier was designed by Dempsey (1997) to overcome the limitations of strain gauges in stiff bridges. His purpose was converting axial strain in a portion of the bridge into a greater bending strain in the amplifier. As shown in Figure 4.5, the amplifier is

composed of two separate parts: an instrumented aluminium beam and a bar inducing an imposed displacement at midspan of the beam.

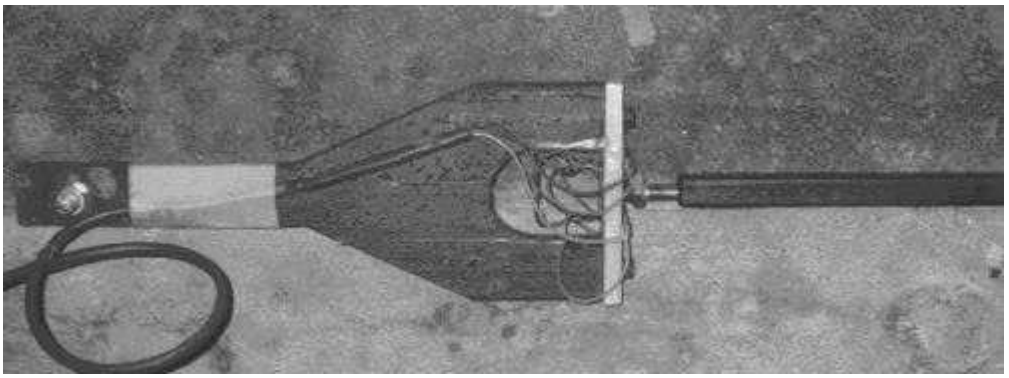

Figure 4.5 – Irish mechanical strain amplifier

Assuming the beam is fixed at the ends, the approximate degree of amplification can be derived from the following formula (González 1996):

$$Amplification = \frac{L_m^{\ 2}}{12 h_m d_m} \tag{4.3}$$

where L_m, h_m and d_m are defined in Figure 4.6.

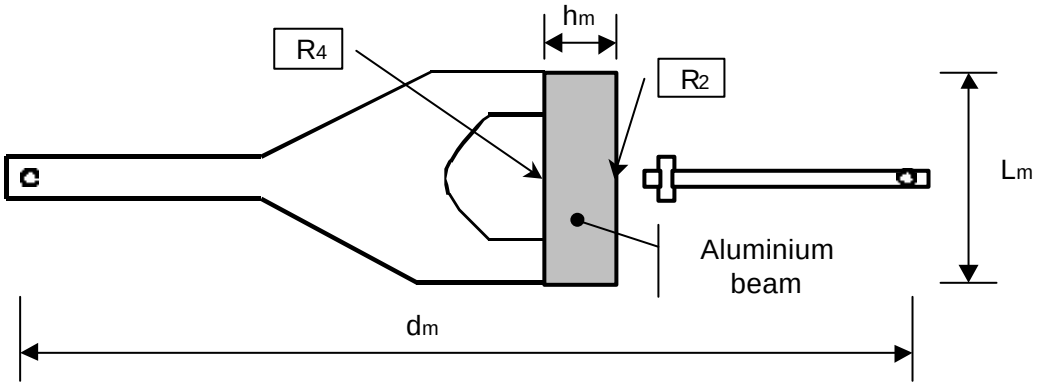

Figure 4.6 – Parameters of Irish mechanical strain amplifier

The original amplifier has dimensions L_m = 60 mm, h_m = 6 mm and d_m = 400 mm, which is equivalent to a strain about eight times bigger than gluing a gauge directly onto the bridge. Strain gauges in compression and tension in Figure 4.6 have the same nomenclature, R_2

and R_4, as in Figure 4.3(b). R_1 and R_3 in this scheme would be fixed resistors in the module block (Appendix C) to complete a half Wheatstone bridge. This is the configuration originally used in the first experiments carried out by the Irish team. Strain in such a configuration is given by:

$$\varepsilon = \frac{-2\left(\frac{e_i(unstrained) - e_i(strained)}{e_o}\right)}{GF}\left(1 + \frac{R_L}{R_2}\right) \tag{4.4}$$

where symbols have the same meaning as in Equation 4.2.

As mentioned in the preceding section, amplification can be improved by the use of four active gauges. In this case, the sections at both supports of the aluminium beam would be instrumented. To achieve this, R_2 and R_4 would be located on compression and tension sides respectively in the section at one support of the aluminium beam, and R_1 and R_3 would be located in a symmetric manner at the other support. The amplifier in Figure 4.5 has this type of installation. This full bridge was used in the experiments that took place place in Luleå, Sweden, and Delgany, Ireland, which results are analysed in Chapter 8. In the case of a full Wheatstone bridge, strain (ε) is given by:

$$\varepsilon = \frac{e_i(unstrained) - e_i(strained)}{GFe_o} \tag{4.5}$$

where e_i, e_o and GF are measured voltage, excitation voltage and gauge factor respectively.

4.3 AXLE DETECTION HARDWARE

Axle detectors, which are mounted on or embedded in the pavement, provide information on speed, axle spacing and vehicle classification. This information is used to locate the truck on the bridge when applying a B-WIM algorithm; the detectors are most conveniently placed at a close distance prior to or on the bridge. Section 3.5.1 describes how sensitive the inferred axle weights are to the axle detector measurements. Fortunately this problem is not as important now since the recent use of optimisation techniques for some bridges to improve initial estimates of vehicle location and speed. Nonetheless, even

for suitable bridges, a good approximation in the initial value of speed is still required to find the true solution (Section 3.5.3).

From the point of view of durability, axle detectors represent the most vulnerable part of any B-WIM system, especially in harsh climates. New developments propose their replacement by appropriate strain readings from underneath the structure in some specific bridges (FAD). The initial estimates of axle location and speed from FAD are not as accurate as from direct measurement, but they benefit from optimisation to improve their results after a few iterations. These systems offer a solution in sites where road surface installations are not feasible (e.g., due to a very thin pavement, a necessity to guarantee waterproofing of the bridge deck, etc.).

4.3.1 Road Sensors

A single sensor can be used for axle counting. Two road sensors, placed at a known distance apart (between 2 and 5 m typically), can accurately measure speed and axle spacings by time and distance (Figure 4.7(a)). By setting two sensors at right angles to the traffic flow, and one other at a known angle between the two (e.g., 45°), it is possible to estimate the lateral position of each vehicle across the road and the width of vehicle.

Removable Sensors

Removable sensors can be pneumatic tubes or tape switches. Both types are placed on the road surface and they are more economical than a permanent solution. Their installation requires less time and traffic delays than other sensors embedded in the pavement, and in certain circumstances, they could be placed without the need for a road closure. However, they are more exposed to traffic aggressiveness and they are not recommended in sites with high traffic densities.

Tape switches are composed of a pair of steel strips, one above the other and held apart by rubber spacers, laid across the road surface. Each time a vehicle’s wheel crosses the detector, the two strips are pressed together thus completing an electric circuit which is detected at the roadside. Compared to pneumatic tubes, they have a shorter life and an extra cost that is justified by the possibility of placing them in a single lane transferring the signal across other lanes through a wire. They are often used for limited duration surveys

and on low volume roads. The road surface is heated before placing the tape switch, and once it is on the ground, it is overlain by an adhesive tape that protects it and keeps it in position.

Pneumatic tubes are thick-walled rubber tubes mounted on the road surface. One end has an air-plug while the other end finishes in a converter that translates the pulse of air caused when the tube is squashed by a wheel into an electrical signal. The tube must be firmly fixed to the road to avoid being whipped up by passing vehicles and thus triggering multiple signals each time an axle crosses. Clamps at the roadside fix these tubes and asphalt-based tape can be used to reassure their location and protect them (Figure 4.7(b)). The air switch should be calibrated so that it is sensitive enough to detect all vehicles irrespective of speed but not so sensitive as to pick up reflected air pulses in the tube.

(a) Layout of axle detectors (b) Detail of a pneumatic axle detector

Figure 4.7 – Axle detectors mounted on the road surface (after Jacob et al. 2000)

An excitation voltage of 5 V or less is required by the pneumatic converter from Golden River[12] used by the Irish team. The voltage measured for the crossing of a 4-axle truck at a scanning frequency of 250 Hz is given in Figure 4.8. Section 4.5.3 gives details how specific software is used to obtain axles from this signal.

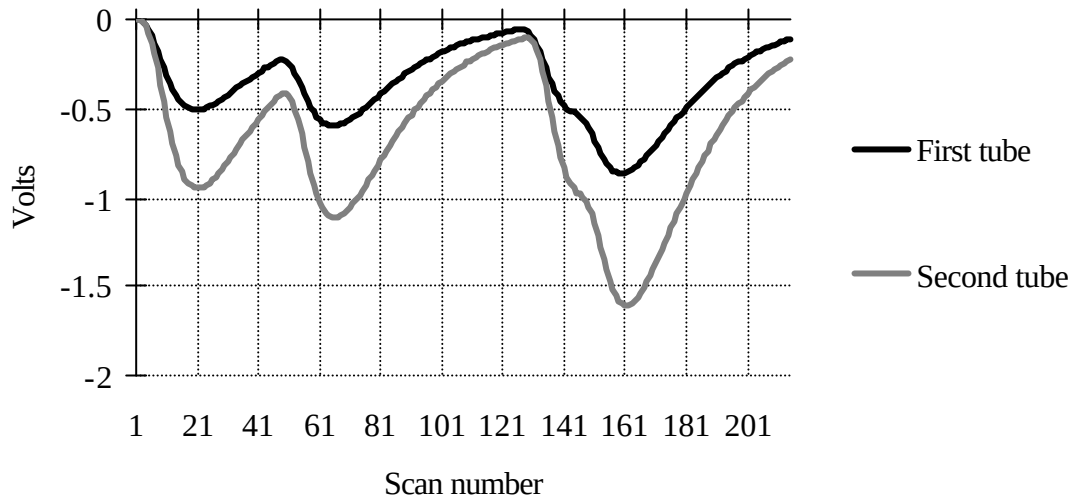

Figure 4.8 – Voltage Signal from rubber tubes at the start and at the end of the bridge

Both types of portable axle detector have been problematic due to the recording of multiple pulses from single axle events and also the missing of some axle events. This is the reason why the Irish team recorded all information in voltages and developed a post-processing algorithm to analyse subsequently those cases considered suspect, i.e., cases for which there was different numbers of axle in each road sensor.

Permanent Sensors

Various types of multicore cable have been developed as an alternative to pneumatic tubes and contact strips laid across the road surface. The most commonly used, known as a tribo-electric cable, contains cores which induce a charge when they rub together and the cable is temporarily distorted by the passage of a vehicle. An increasingly popular variant on this is the piezo-electric cable which contains piezo-electric material such as polarised ceramic powder. A coaxial-conductor attached to the piezo-electric cable (Figure 4.9(a)) is subject to an electrical charge when the piezo is squashed. The housing should be impervious to attack from acids, alkalis, salts and ultraviolet light. All connections are fully sealed within the housing as shown in Figure 4.9(b).

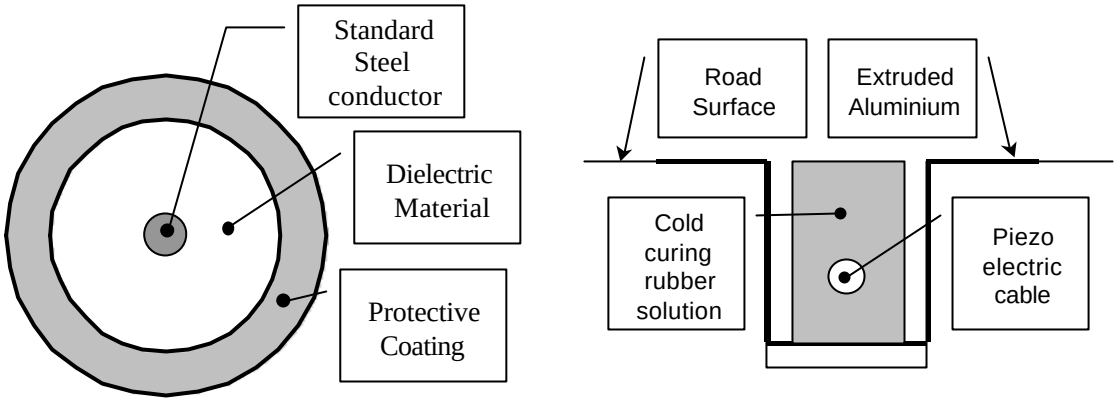

(a) Piezo-electric cable (cross section)

(b) Permanent installation of piezo electric cable in a slot (cross section)

Figure 4.9 - Piezo-electric axle detector

These axle detectors lie across the carriageway. They are all triggered by the passage of vehicle wheels and thus produce a count of axles rather than vehicles. They must be installed at right angles to the flow (otherwise they might detect two wheels on one axle as if they were separate axles) and this effectively prevents their use for counting axles of vehicles undertaking turning movements. Top grade piezo-electric cable is relatively expensive and needs careful installation and calibration but, since the change in signal is proportional to the load applied, it can be used for classifying vehicles according to their weight.

A BNC (**B**ayonet **N**ut **C**onnector) connector is fitted to the end of the coaxial cable with adequate stripping and cramping tools. This BNC connector is plugged into an interface that converts a very noisy input signal into a clean output pulse identifying the axle presence that will be recorded by the data acquisition system. The interface used by the Irish team is the T2000.44, a dual channel piezo-signal conditioning circuit, mounted on a printed circuit board developed by Traffic 2000. The interface gives a pulse width of 20 mS (adjustable) for every axle passage. Figure 4.10 shows the signal provided by the piezo-electric sensor interface at a scanning frequency of 1000 Hz. Each rectangular pulse represents an axle.

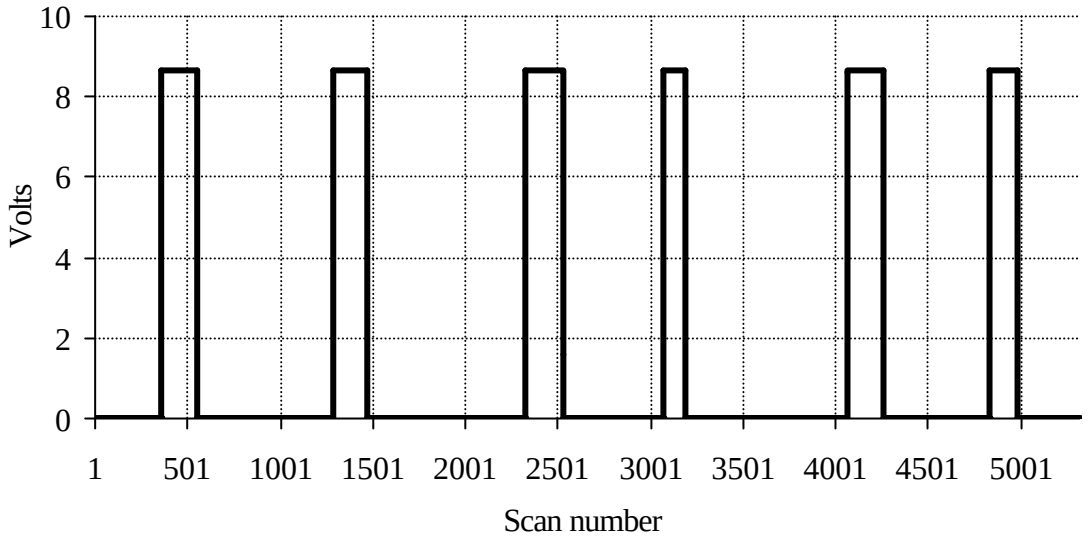

Figure 4.10 – Signal provided by piezos installation

Though piezoelectric axle detectors embedded in a groove in the road generally provide a longer life than those mounted on the road surface, they can fail in various ways:

- Total break in piezo cable or signal cable → No output.
- Joint failure → No output.
- Water in joint → Gradual increase in noise until it exceeds threshold leading to eventual failure through noise.
- Failure of piezo cable in body of sensor but core held together by elasticity of rubber → Very unusual indeed. Intermittent output.
- Poor BNC connection resulting in corrosion and build up of oxidation → Reduced output and intermittent.
- Poor BNC connection central core pin not driven home → Possible intermittent.

4.3.2 FAD Systems

One of the main problems with B-WIM installations is the longevity of axle detectors mounted on the road surface. These detectors are rapidly destroyed by heavy traffic. They also warn drivers about the presence of instrumentation on the bridge.

LCPC (**L**aboratoire **C**entral des **P**onts et **C**haussées) first considered the idea of using a B-WIM system without axle detectors as a requirement to ensure the waterproofing of the deck in the Pont de Normandie. Dempsey et al (1998a) and Žnidaric et al (1999a) studied

the performance of FAD systems for orthotropic and short slab bridges respectively. Two different longitudinal measurement locations are required to calculate velocity and axle spacings. Figure 4.11(a) shows FAD instrumentation at one section for an orthotropic bridge; the complete system consists of sensors at two such sections between transverse beams. Figure 4.11(b) shows the corresponding installation for a short slab bridge, where sensors are normally located around ¼ and ¾ of the span.

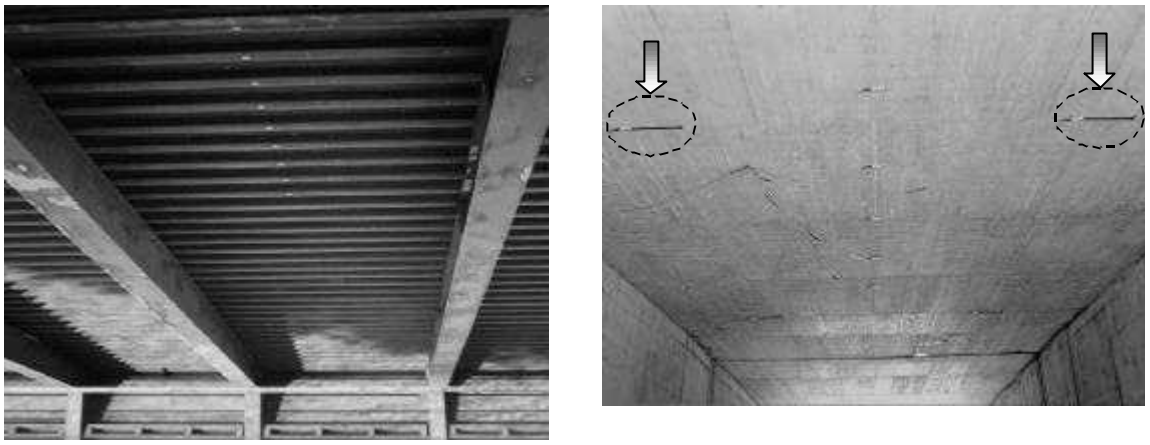

(a) Orthotropic Bridge Deck (b) Short Span Slab Bridge

Figure 4.11 – Installation for a Free Axle Detection System (after Jacob et al. 2000)

Principle

Bridges that qualify for FAD allow easy identification of axles from strain peaks. The exact location of these peaks can be obtained from the first derivative of strain with respect to time. If sensors are placed at two different longitudinal locations, it is possible to obtain velocity and axle spacings solely from strain records.

Velocity is readily calculated from geometric distance between sensors and time, Δt, taken by the vehicle to cross the sensors. In orthotropic bridges, Δt (Figure 4.12) is obtained from minimising an error function given by the squared difference between the strain in the first longitudinal location at time t and the strain in the second longitudinal location at time $t + \Delta t$ (Dempsey et al 1999b).

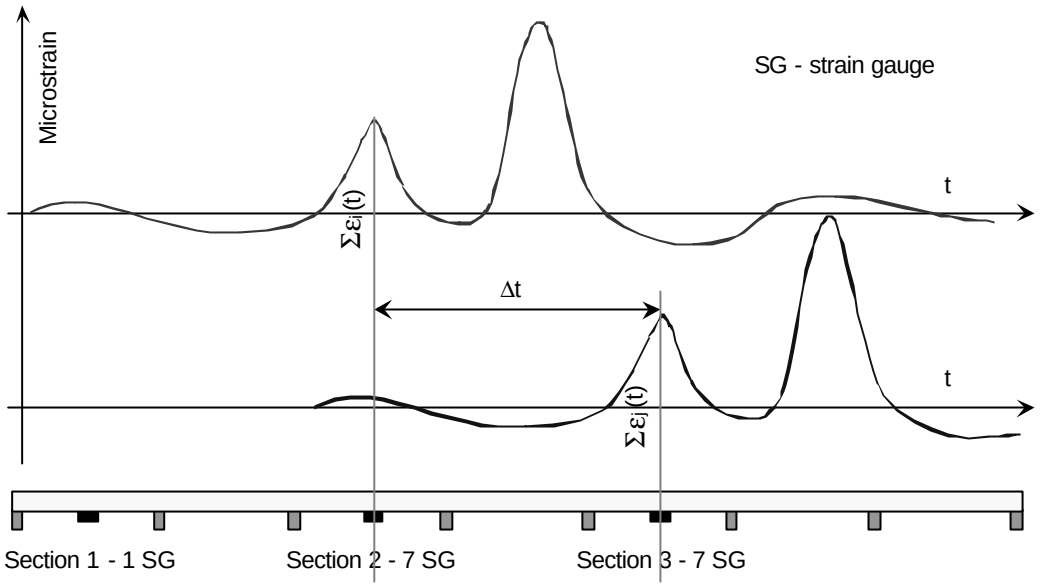

Figure 4.12 –Response to the passage of a 2-axle truck over an orthotropic deck (after Dempsey et al. 1999b)

Ideal Site

Axles are easier to identify in the strain record when they produce sharp peaks. The shape of the strain response depends on several factors:

- The shape of the influence line (Figure 3.5).
- The span length and axle spacings. Longer instrumented spans make it more difficult to distinguish individual axles. Figure 4.13 shows the response of an 8 m long integral bridge and a 32 m bridge to the passing of 5-axle semi-trailer. When looking at Figure 4.13(a), there are clear sharp peaks for individual axles, even the rear closely spaced axles of the tridem. In contrast to this response, the first mode of vibration of the long bridge prevents the identification of axles in Figure 4.13(b) and it does not qualify for FAD.
- The thickness of the instrumented superstructure. Thin superstructures provide sharper peaks, while greater depths smooth peaks out.

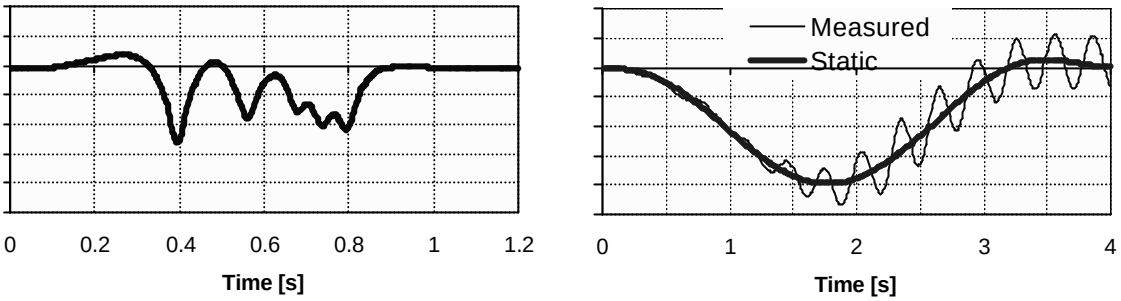

(a) Response of an 8 m long integral slab bridge

(b) Response of a 32 m long simply supported beam bridge

Figure 4.13 – Strain response for different bridge lengths (after Ž nidaric et al. 1999a)

Jacob et al (2000) propose a coefficient to determine if a site qualifies for FAD. This is given in Equation 4.6:

$$C_{FAD} = \frac{Lh}{d_{\min} f_i} \tag{4.6}$$

where L is the span length, h the superstructure thickness, d_{min} the minimal axle spacing and f_i a factor depending on the influence line as defined in Figure 4.14.

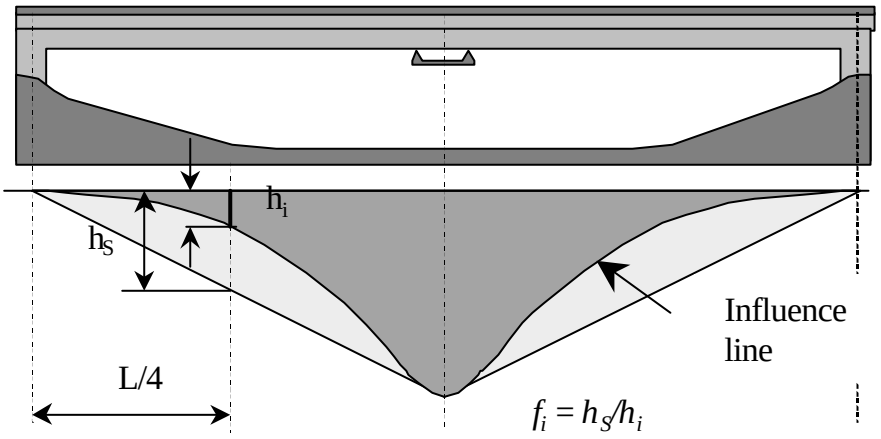

Figure 4.14 – Definition of f_i (after Jacob et al. 2000)

First studies by Jacob et al (2000) indicate that the following bridges qualify for FAD:

- Short span, frame-type slab bridges with $f_i \cong 3$ and $1 < C_{FAD} < 2$.

- Longer span bridges with a thin slab supported in the lateral direction by cross beams or stiffeners (i.e. orthotropic bridges) with $C_{FAD} < 0.5$.

Theoretical Testing

Experimental results for orthotropic decks have been given in Section 3.7.3. The possibility of extending FAD systems to other bridge types can be investigated with theoretical dynamic models. Dempsey et al (1999b) use two different theoretical models to test the FAD algorithm: A finite element model and a one-dimensional numerical model as proposed by Frýba (1972). This numerical approach will be discussed in Chapter 5. It was found good agreement between Frýba and finite element models. Strain results are analysed for three bridge span x width dimensions (5x8.5, 10x8.5 and 20x8.5 m), two boundary conditions (fixed-fixed and simply supported), and one vehicle (12 tonnes gross weight), whose characteristics are described below.

In this analysis, the author developed the finite element model using the MSC/NASTRAN software[18]. The bridge and vehicle models are represented in Figure 4.15.

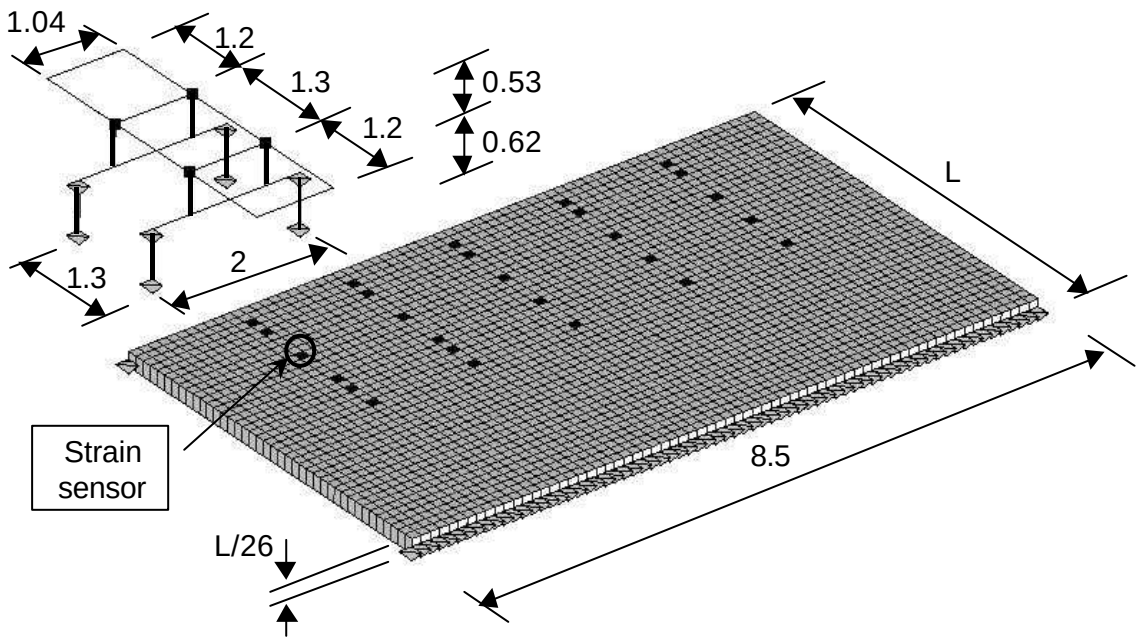

Figure 4.15 – Bridge-vehicle finite element model

The dynamic interaction of the bridge and the vehicle incorporates the road surface profile and it is implemented using a set of auxiliary functions to enforce the compatibility

conditions at the bridge/vehicle interface (Cifuentes 1989). Accordingly, software was developed to generate an entry into the assembled stiffness matrix of the vehicle-bridge system. This entry allows for the definition of the forces acting on the bridge due to the moving wheels and the equation of motion of the vehicle. A compatibility condition between the vertical displacement of the wheel and the bridge at the contact point is also established. This formulation is explained in detail in Chapter 6. In order to determine the most suitable locations for the position of the sensors, strain was obtained at seven longitudinal (1/16, 1/8, 1/4, 5/16, 3/8, 7/16 and ½ of the span length) and five transverse locations (sensors represented in black in Figure 4.15).

The bridge structure was fixed at both ends to simulate the conditions in an integral bridge. The section was made of an isotropic material of $36x10^9$ N/m^2 Young's modulus, 2.45 t/m^3 unit weight, and uniform thickness taken as 1/26 of the bridge length. The first longitudinal and torsional natural frequencies were 30.9 and 33.07 Hz in the 5 m span (Figures 4.16), 15.4 Hz and 19.37 Hz in the 10 m span, and 7.66 and 13.78 Hz in the 20 m span bridge. Damping was taken as 1% in all cases.

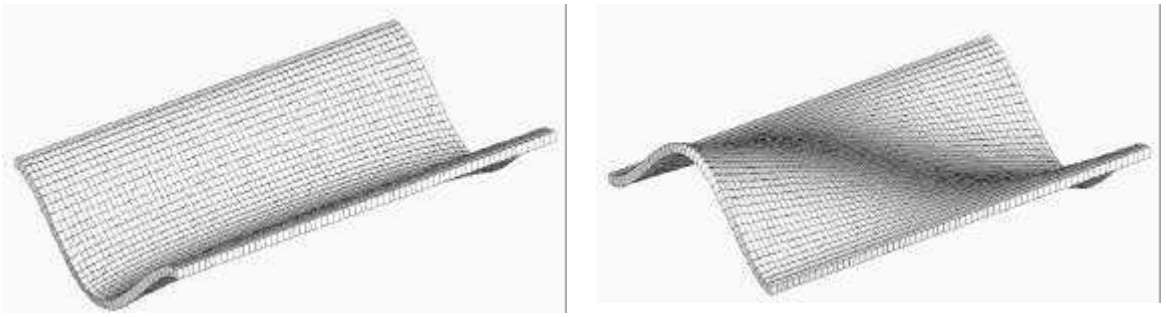

(a) First mode shape (30.9 Hz) (b) Second mode shape (33.07 Hz)

Figure 4.16 – Bridge mode shapes (5 m span)

The vehicle was modelled as a rigid frame tandem with 1.3 m between axles (distinguishing between axles of a group is one of the greatest challenges in FAD systems). The tandem speed was 20 m/s and it was excited by the road roughness in the approach prior to the bridge. Road irregularities were idealised as a stochastic process and generated from power spectral density functions for 'good' conditions (Wong 1993). The inner and outer wheels followed a path 1 m and 3 m offset from the bridge centre line (Figure 4.15). The mass of each axle was 10^3 kg and the mass moment of inertia 600 kgm^2. A frame weighing 10^4 kg connected both axles. The suspension was modelled with spring and

damper elements at each wheel of values $1.8*10^6$ N/m and $5*10^3$ Ns/m respectively, while each tyre had a stiffness $2*10^6$ N/m and damping $3*10^3$ Ns/m (Kirkegaard et al. 1997). The main truck frequencies were 1.65 Hz body pitch (Figure 4.17(a)), 2.03 Hz frame twist (Figure 4.17(b)), 2.92 Hz body roll, 3.02 Hz body bounce, 13.96 Hz axle hop (out of phase), 14.19 Hz axle hop (in phase) and 16.84 Hz axle roll (out of phase).

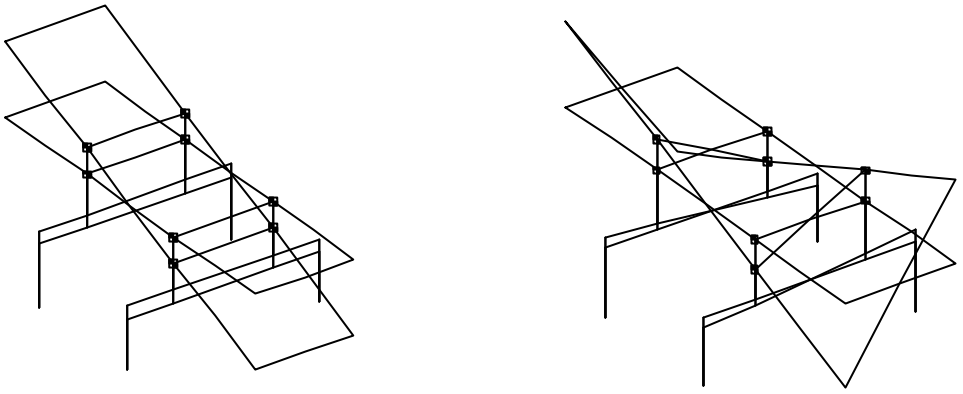

(a) Body pitch (1.65 Hz) (b) Frame twist (2.03 Hz)

Figure 4.17 – Truck modes of vibration

Figure 4.18 illustrates the response of the bridge to the passage of the tandem at different longitudinal locations (strains at different transverse locations are added up). From this figure, the ideal location of the FAD sensors for axle detection is between L/4 and 3L/8.

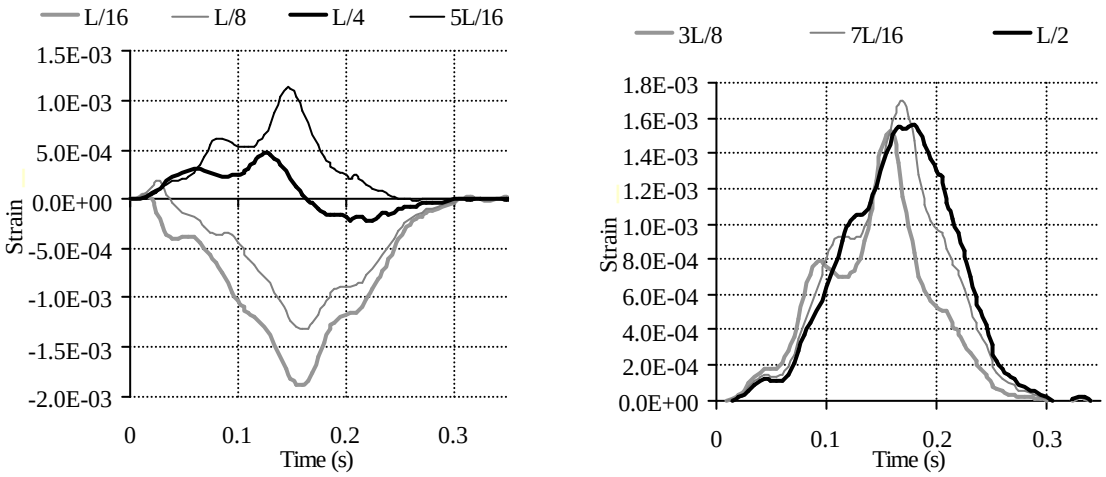

(a) Response at L/16, L/8, L/4 and 5L/16 (b) Response at 3L/8, 7L/16 and L/2

Figure 4.18 – Response at different longitudinal sections in the case of 5 m span length (L) to passage of tandem

Figure 4.19 shows the individual responses of strain gauges at different transverse positions for a longitudinal position at ¼ of the span length for the 5 m bridge. It can be seen that the axles of the tandem are far more distinct than in Figure 4.18 and that some transverse positions are clearly better than others (strain from sensors in Figure 4.18(b) is worse than Figure 4.18(a) for axle identification).

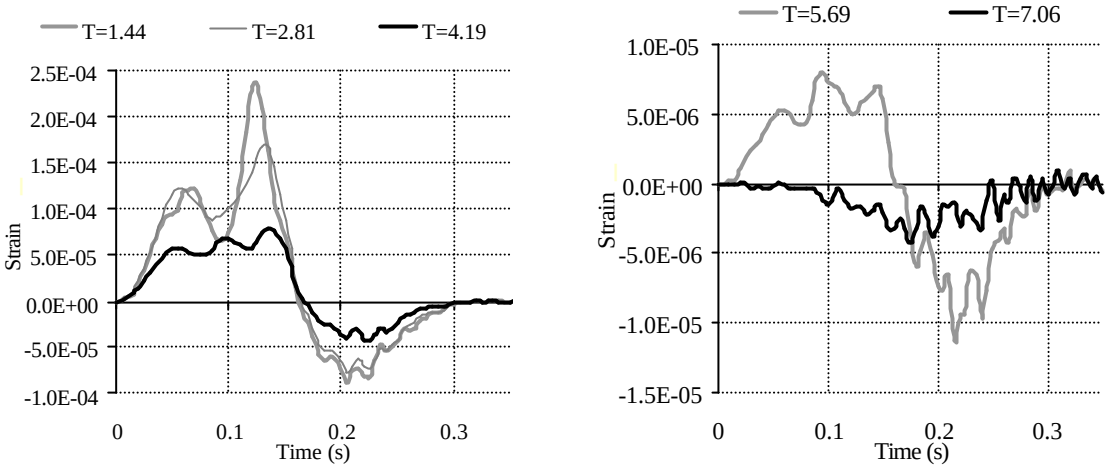

(a) Response at T=1.44, 2.81 and 4.19 m (b) Response at T=5.69 and T=7.06 m

Figure 4.19 – Response at ¼ of span length at different transverse locations in the case of 5 m span length (T is distance in m from the edge of the bridge driving lane)

Figures 4.20 shows the response of the 10 m bridge. From the seven longitudinal positions, axle peaks are easier to identify at L/4.

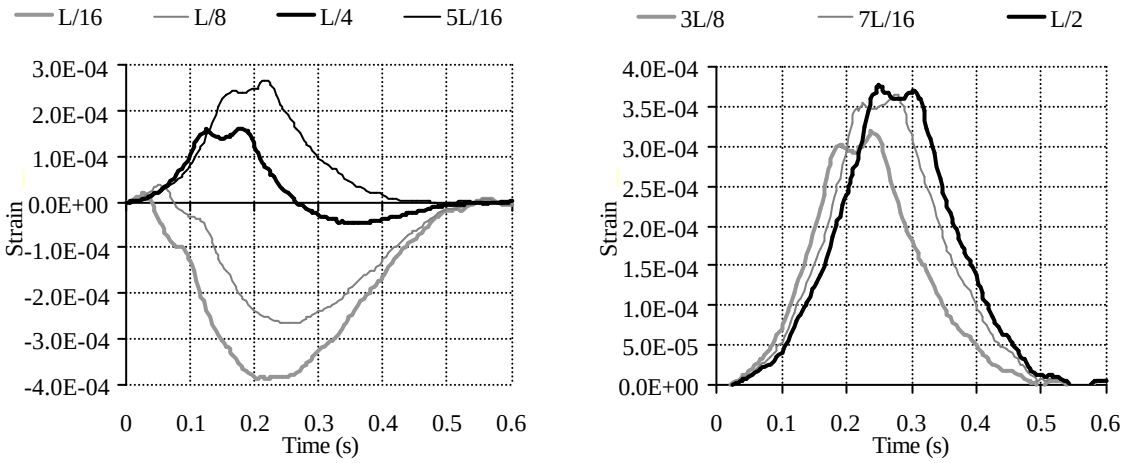

(a) Response at L/16, L/8. L/4 and 5L/16 (b) Response at 3L/8, 7L/16 and L/2

Figure 4.20 – Response of 10 m span (L) bridge to passage of tandem

Figures 4.21 shows the response of the 20 m bridge. In the 20 m bridge studied in this paper, the in-phase and out of phase axle hop frequencies dynamically excite the first torsional mode of the bridge, interfering with the static response and making it impossible to use for FAD purposes.

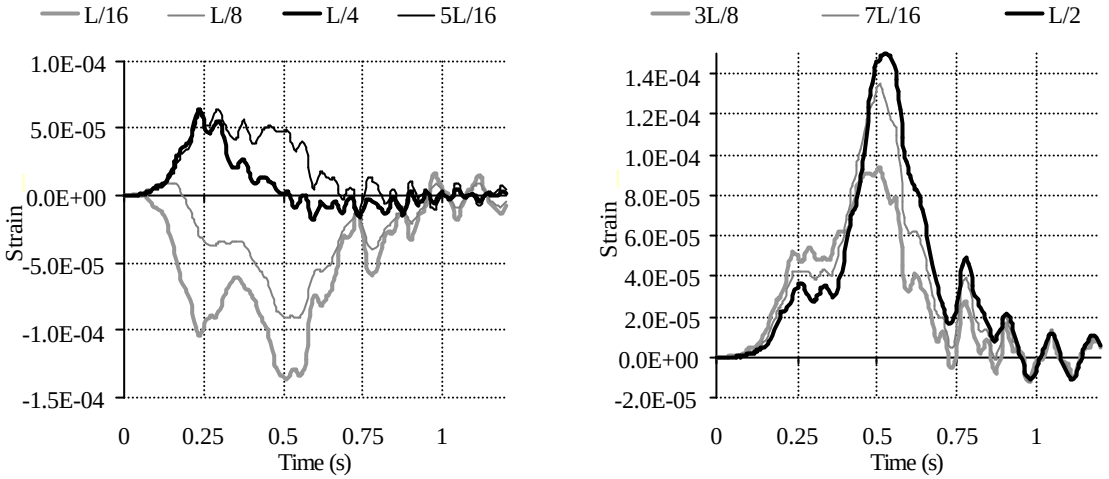

(a) Response at L/16, L/8. L/4 and 5L/16 (b) Response at 3L/8, 7L/16 and L/2

Figure 4.21 – Response of 20 m span (L) bridge to passage of tandem

As result of this study, the author in collaboration with others (Dempsey et al.1999b) makes the following recommendations:

- In the case of a simply supported bridge, the FAD algorithm is only suitable for spans shorter than 5 metres and both longitudinal sensor locations must be close to the supports, e.g., L/16 and L/8.
- In fixed-fixed bridges, a maximum span of 10 m or even greater is possible if it is proven that the total bridge response is not modified significantly by its dynamic interaction with the vehicle. Both axles of the tandem were identified in the 5 (Figure 4.18) and 10 m bridge (Figure 4.20). Velocity is better determined for an average longitudinal location of L/3 as illustrated in Figure 4.22(a).
- Velocity is more accurately defined for increased distances between sensors (Figure 4.22(b)) and increased scanning frequency. A minimum longitudinal distance between sensors of 1 m and a minimum scanning frequency of 200 Hz should be considered.

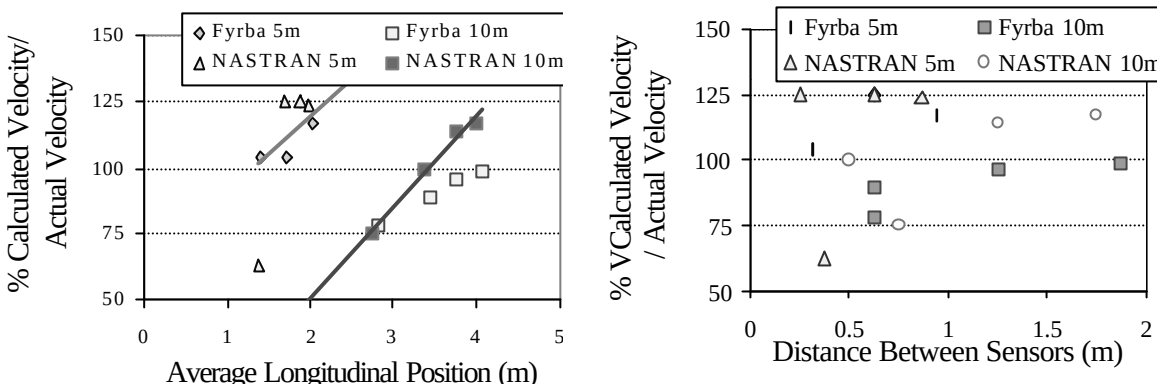

(a) Longitudinal Position of Sensors (b) Inter-sensor Distance

Figure 4.22 – Accuracy of calculated velocity from FAD algorithm for 5 m & 10 m bridges (after Dempsey et al. 1999b)

4.4 SOFTWARE

The software of a B-WIM system can be divided into two main parts: DAQ software and software for determination of axle weights. DAQ software integrates the strain signal, signal conditioning and DAQ hardware to provide a reliable input to the software that calculates the characteristics of traffic.

4.4.1 CULWAY

CULWAY is a high speed weigh-in-motion system that uses existing box culverts to automatically and unobtrusively monitor traffic. It can calculate accurate data for all vehicles travelling up to 150 km/h in up to 4 traffic lanes simultaneously, 24 hours a day with no operator required. It was developed by Peters (1986) of Main Roads, Western Australia and subsequently developed as a commercial product by ARRB Transport Research with substantial and ongoing input from all Australia State Road Authorities[10].

The CULWAY procedure to calculate weights has been described in Section 3.4.2. This system reports automatically via fax about: Data on weight - no. of axle groups, speed - axle group weight, length - axle spacings, width - tyres per axle, no. of axles - vehicle lane position. The first CULWAY system (Figure 3.4(b)) was programmed to work unattended by following the flow chart shown in Figure 4.23 (Peters 1986).

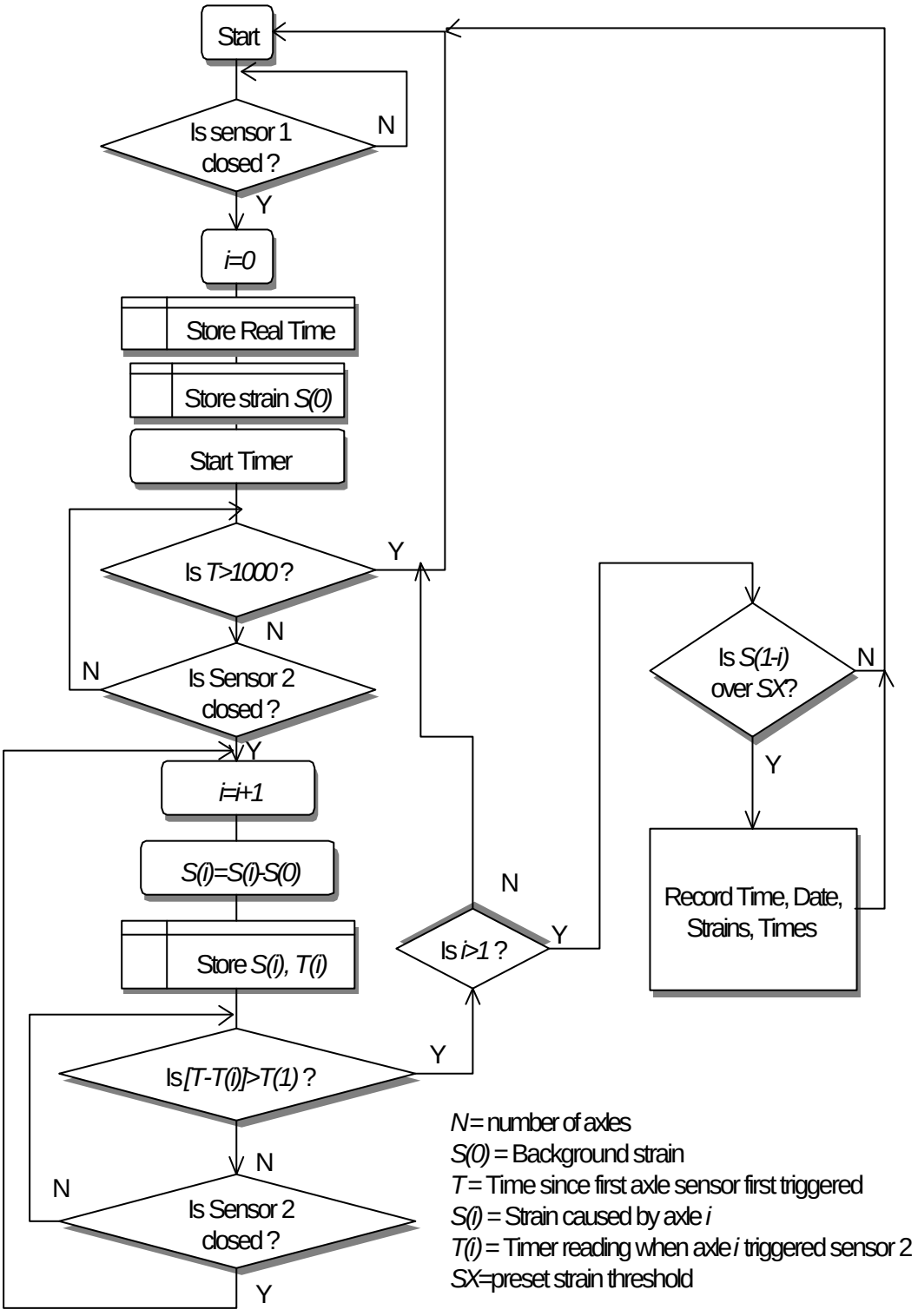

Figure 4.23 – CULWAY Flowchart

4.4.2 SiWIM

SiWIM is a Weigh-in-Motion program developed at ZAG, a research institute in Slovenia, within the framework of WAVE. The program runs in any 32-bit Microsoft Windows

environment. SiWIM uses National Instruments data acquisition products. Currently it supports two PCMCIA cards. When acquisition starts, depending on the choice, either the data acquisition device is initialised or an existing file is opened for input. The format in both cases is the same. Then, the data from the PCMCIA or the file is put into an internal queue. After saving this queue in a new file, data can be filtered in several ways. The filtered data is transferred to another queue from where it will be read for vehicle detection. There are two different options for vehicle detection: (a) based on signals from axle detectors mounted on the road surface or (b) based on signals from strain sensors (FAD). Data is stored in an internal queue until the last axle of the vehicle leaves the bridge. All this information can be fed to a preprocessed data queue or saved for later processing. The calculation of weights can be done with either an internal or an external algorithm. In the latter case, the pre-processed data is written into a file and a predefined executable file is called to calculate axle spacings and weights. The internal algorithm uses a development of Moses' approach for this calculation (Moses 1979). Finally, the initial results are refined through the application of an optimisation algorithm. Once results are obtained, they are displayed on the screen and, optionally, written to a file. Figure 4.24 shows how this system can also incorporate FAD technology.

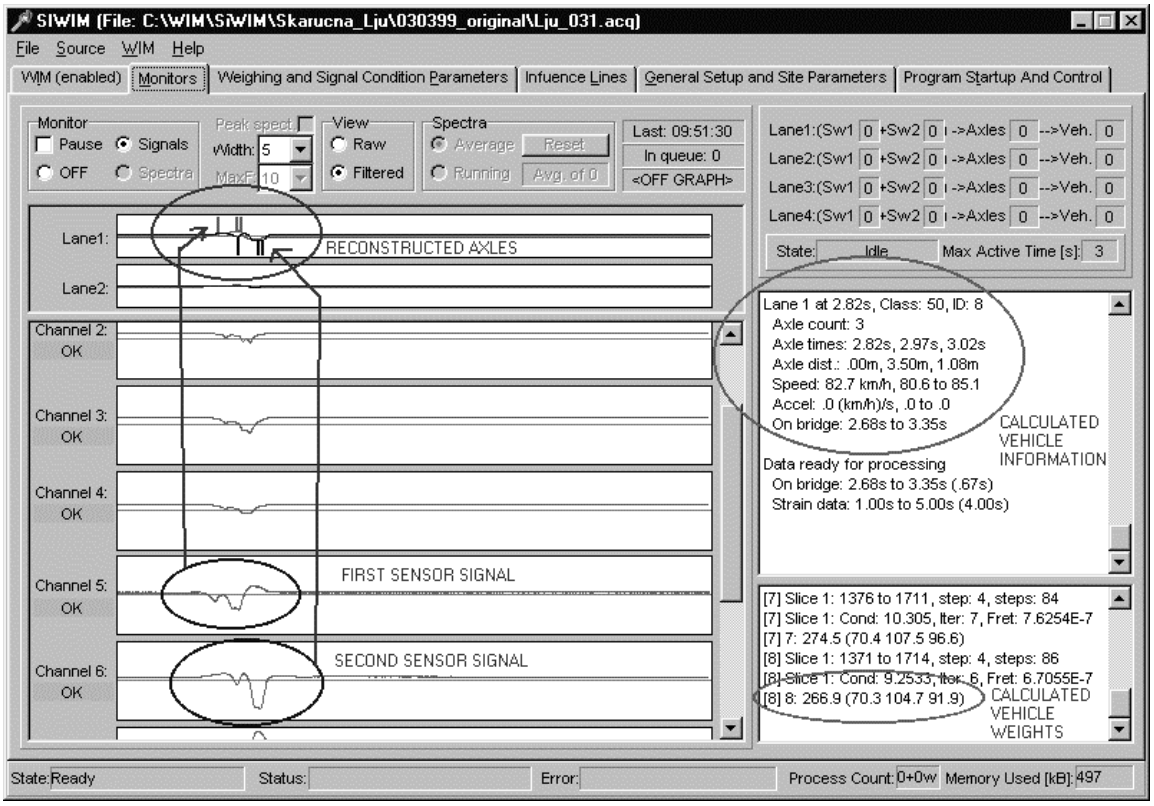

Figure 4.24 – SiWIM software (after Jacob et al. 2000)

WIMDAP© (Ž nidaric et al. 1998) is another software developed at ZAG to correct the theoretical influence line by adjusting the boundary conditions of the span according to the guidelines given in Section 3.5.1, and smoothing the peaks to account for the smeared footprint of the tyre. Figure 4.25 shows the interface of this program.

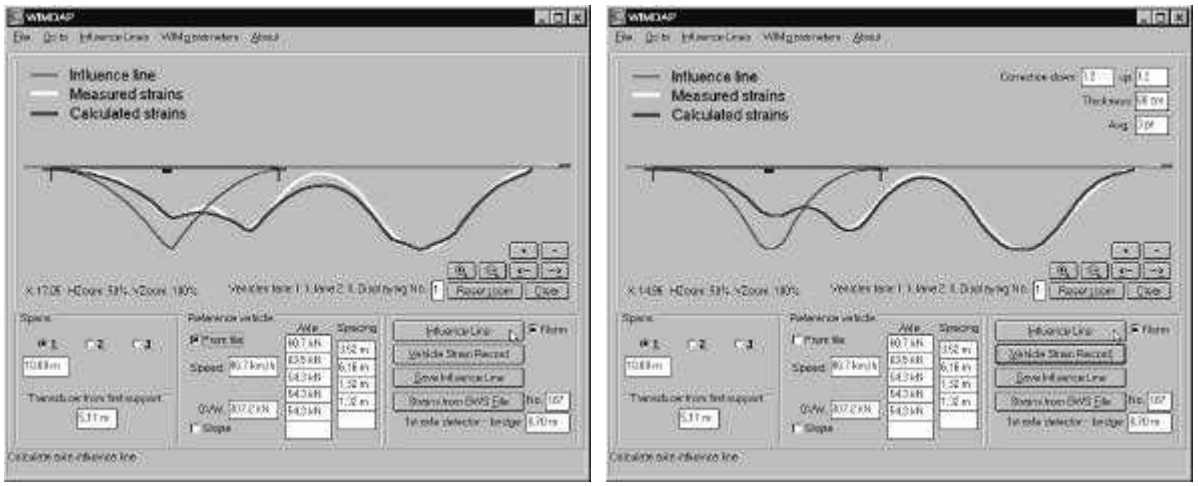

(a) Theoretical influence line (b) Optimised influence line

Figure 4.25 – Adjustment of the influence line in WIMDAP© software (2S3 semi-trailer) (after Ž nidaric et al. 1998)

4.4.3 Irish B-WIM

Labview software[14] was used during data acquisition while post-processing was programmed in the C language[15]. The Labview programs to record voltage from axle detectors and strain sensors were written by Kealy (1997). The author developed C code to convert that information on voltages into vehicle classification and weights. First, the original voltage information is converted into times and strains for every vehicle. There is a time stored for each axle at each tube and strain is recorded while there is traffic on the bridge. After obtaining vehicle classification and speed, weights are calculated by applying Moses' static algorithm (Section 3.3).

Data Acquisition

Information on voltages can be acquired in two different ways: one writes data to a binary file (Figure 4.26(a)) and another to an ASCII file (Figure 4.26(b)). The latter allows graphical output and checking of the system in real time, but it requires more storage space.

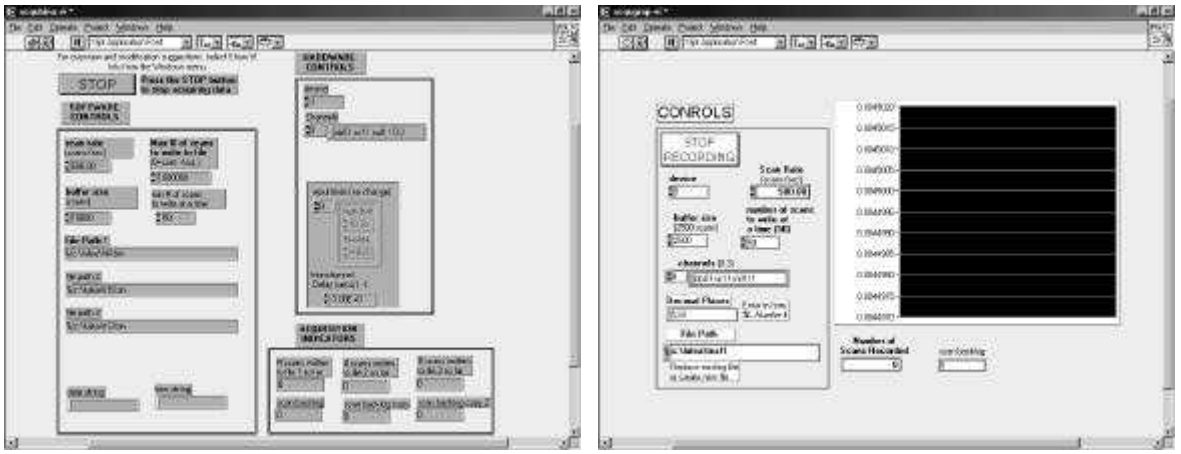

(a) Collection of Data in Binary Format (b) Graphical Collection of Data

Figure 4.26 – Data Acquisition Programs

The binary format is generally used when collecting data for long uninterrupted periods. If binary format is recorded, another Labview program allows a posterior conversion into text format. The two DAQ Labview programs use a circular buffer technique that continuously acquires data at the same time as retrieving and writing previously acquired data to a file. The input of these DAQ programs specify:

- DAQ card (see Appendix C).
- Number of scans per channel per second for all listed channels.
- Channels on the SCXI (**S**ignal **C**onditioning e**X**tensions for **I**nstruments) hardware that are to be scanned and to which channels on the DAQ card they are to be written (see Appendix C).
- File into which the acquired data is to be written.
- Minimum number of scans to be read from the buffer on each iteration. It is recommended as half the scan rate.
- Maximum number of scans which can be held in the circular buffer. It should be set to at least 0.75 times the scan rate.
- Maximum number of scans to write to each file, so a new file is created when the previous file reaches this limit.
- Time delay between scanning of two successive channels.
- Range of input voltages. If left empty values default to hardware settings.

Axle detection algorithm

Accurate speed and axle spacing are essential for a B-WIM algorithm. Small errors in axle spacing, and especially in speed, result in large errors in axle weights (Dempsey 1997). Initially the system was controlled through software written in C++ (O'Connor 1994) using rubber tubes fixed to the road with asphalt tape. This program controlled the whole data acquisition, as strains were only recorded when there were axles on the bridge. The disadvantage of such an approach is that an error in the axle detection device leads to loss of strain data. Problems with the tubes attached to the road in the Delgany site (Section 8.2) resulted in the purchase of new axle detectors: tape switches. However, tape switches gave multiple signals for just one axle hit and sometimes collapsed under the weight of the vehicles. Five different tape switches with different time delays were used, but none of them gave good results after the second day of use (González 1996). Finally, it was decided to record all data continuously and to process it afterwards in the laboratory. Pneumatic tubes taped to the road were again used but, this time, the voltage signal from the pneumatic convertor was monitored and stored during the data acquisition exercise (Kealy 1997). These changes provided access to both raw and processed signals facilitating the resolution of likely conflicts after processing. The voltage signal was converted into axle hits using purpose-written software run afterwards in the laboratory. This corrected most of the problems related to axle detection. Rubber tubes attached to the road with clamps were also used as axle detectors. As they tended to get loose, they were firmly fixed every two days to ensure an uninterrupted record. Several video records with a variety of different truck configurations and the corresponding tube signals were collected on site to check the reliability of the new system and it was found to operate quite effectively.

Considerable effort was expended by the author on the development of software to convert the voltage signal from the pneumatic convertors into times of axle hits. It was first determined that the slope of the voltage curve was clearer than the voltage curve itself, particularly for the detection of tandems. Figure 4.27 illustrates the slopes (first derivatives with time) from two tubes as a four-axle vehicle with a rear tandem passes over. The original voltage signals are shown in Figure 4.8. Further, the absolute magnitudes of voltage (i.e., using high and low values as triggers) were found to be unsuitable as they were dependent on axle weights, vehicle speed, synchronisation of both wheels on the tube, tyre characteristics, etc..

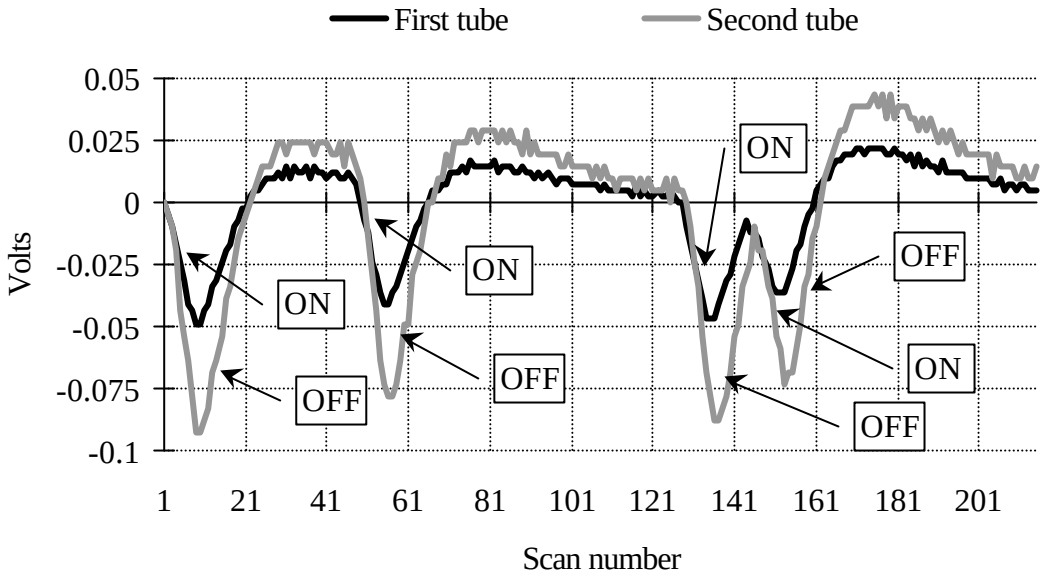

Figure 4.27 – Slope of Voltage signal in Figure 4.8

The following criteria to identify axles were adopted:

- There is a flag for each rubber tube signal corresponding to an axle hit. When the flag goes from OFF to ON, it indicates that there is an axle on the tube.
- The flag changes from OFF to ON if the slope decreases for consecutive *p* scans to ensure it is a truck (Figure 4.27). This number *p* has been adjusted with the sample and it depends on the quality of the voltage signal, the scanning frequency and the length of the tube and wiring. It is a time condition that minimises the influence of axle weight or vehicle characteristics. The assumption is that slope starts to decrease the moment an axle hits it. The inaccuracy is around 1 scan, given by the starting point. The total decrease in slope must be in excess of a certain value which is determined from the sample, and is different for each tube.
- The flag goes from ON to OFF when the slope increases for *p* scans. The same number of scans as before is used as, if there is an axle present after *p* scans, it is reasonable to also say that the influence of that axle hit disappears after another *p* scans. Conditions on the absolute values of the slope are not imposed, as such a condition cannot distinguish between the presence of an axle on the bridge and white noise. The flag also goes from ON to OFF when the slope decreases, but the second derivative increases for *r* scans (Figure 4.28).

The critical number of scans, *p* is needed to avoid the registration of more than 1 axle when only one is present, while *r* ensures axles are not missed in closely spaced configurations. Both temporal parameters are controlled through software. Tests in Delgany, Ireland, took place at a scanning frequency of 250 Hz, and $p = 5$ scans and $r = 6$ scans were adopted, though these values can be adjusted depending on the quality of the voltage signal. In Figure 4.26, which gives first derivative of voltage with respect to time, 5 to 8 scans can be clearly counted when the slope curve decreases in response to an axle.

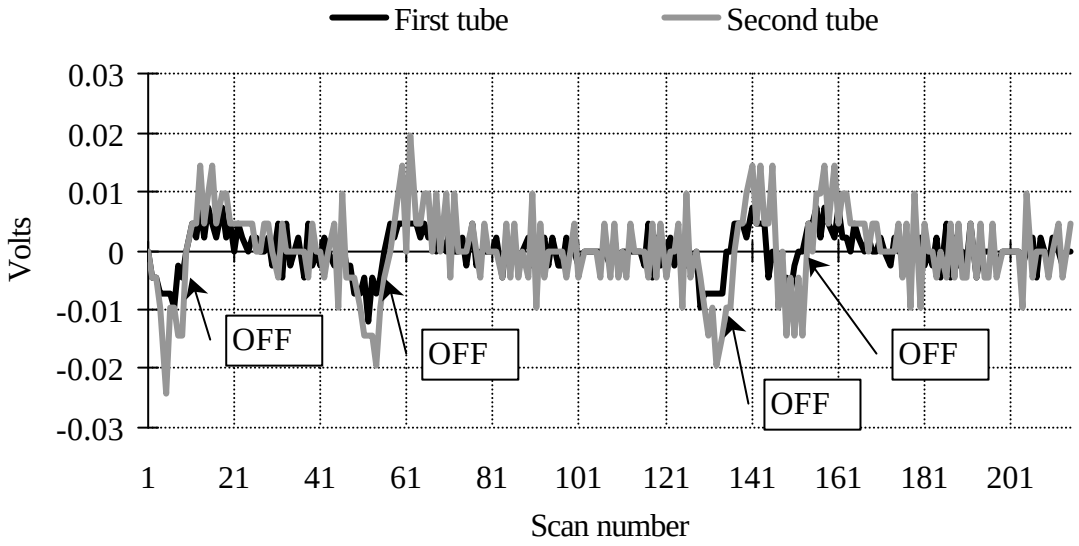

Figure 4.28 – Second derivative with time

Error detection

Sometimes there are anomalies in recordings: i.e., axles read in one axle detector but missed in others. These records are probably due to vehicle lane changes and are removed in weight calculations. The program detects these events by evaluating the number of axles on the bridge from both tubes. The program also compares the axle spacing in scans obtained from the first and second tube. If the difference between these is significant, the event will be marked as doubtful for weight calculation purposes.

Though unlikely, some closely spaced axles could be missed due to an incorrect layout of the tubes. This can occur if the portion of the rubber tube that lies off the road is not straight enough or is too long before being connected to the pneumatic converter. Either of these cases can result in the voltage signal being too weak. Alternatively, an air pulse could reach the detector before the tube recovering normal pressure, making it difficult to

distinguish pulses in the converter signal. For these cases, if one of the tubes failed to identify one axle but the other tube gets it, the axle will be counted as good, as experience confirms that the algorithm works well when a good voltage signal is provided. Given the characteristics of the algorithm, there have never been extra axles reported in a vehicle. The problem in the old system with multiple phantom axles has been solved.

The axle detection algorithm also checks for the maximum number of axles physically possible between rubber tubes. Each time an error is detected, that traffic event is recorded with a character indicating the source of error, and all variables are initialised for counting a new traffic event.

Speed and Distance between Axles

The author studied the best procedure for determining initial estimates of speed and axle spacing. Once the times for each axle at each tube have been obtained, speed and distance between axles can be readily calculated. Speed is considered to be approximately constant in the distance between rubber tubes (assumption also adopted in the calculation of weights), and is obtained by averaging all time references for an axle hit as given in Equation 4.7:

$$v = \frac{NL_t f}{\sum_{i=1}^{N} (q_{i2} - q_{i1})} \tag{4.7}$$

where v is velocity (m/s), q_{i2} , scan number for axle i to touch second tube, q_{i1}, scan number for axle i to touch first tube, f, scanning frequency (Hz), N, number of axles and L_t, distance between rubber tubes.

A degree of uncertainty is involving in the identification of the starting scan of an axle hit. This error is inversely proportional to the scanning frequency. During tests carried out in Delgany, Ireland, with a scanning frequency of 250 Hz and distance between tubes of 22 m, the maximum error in timing was calculated as the time for 1 scan = 1/250 = 0.004 seconds in ideal conditions. At 90 km/h (25 m/s), an axle would take a time of 0.88 seconds to cross between both tubes. If the measured time was 0.004 seconds higher due to the scanning frequency, the measured speed would be 0.44 % smaller. The final error

should be less than 0.44% as the definitive speed of the vehicle is calculated from averaging each axle speed.

Before obtaining axle spacing, the total distance between first and last axle (total wheelbase) is calculated by Equation 4.8:

$$S_{1N} = v\left(\frac{q_{N1} + q_{N2} - q_{11} - q_{12}}{2f}\right) \tag{4.8}$$

where S_{1N} is spacing (m) between 1st and last axle; q_{N1}, scan number at which the last axle hits the first tube, q_{N2}, scan number at which the last axle hits the second tube, q_{11}, scan at which the first axle hits the first tube, q_{12}, scan at which the first axle hits the second tube, and v, velocity, is defined in Equation 4.7.

Axle spacing is assigned based on the relative time interval. For example, the distance between second and third axle is calculated as:

$$S_{23} = \left(\frac{q_{31} + q_{32} - q_{21} - q_{22}}{q_{N1} + q_{N2} - q_{11} - q_{12}}\right) S_{1N} \tag{4.9}$$

where the subscripts have equivalent meaning to those in Equation 4.8.

When calculating axle spacings, errors are reduced by averaging times between axles given by each tube. An error of one scan represents 10 cms for a scanning frequency of 250 Hz and a speed of 25 m/s. A 3-axle truck with axle spacings 4.02 m and 1.2 m, was used to test the approach. Figures 4.29 and 4.30 show the results obtained for axle spacings when applying the axle detection algorithm. It can be seen that the influence of speed on accuracy is negligible between the first and second axle, but significant in the case of the rear tandem illustrated in Figure 4.30.

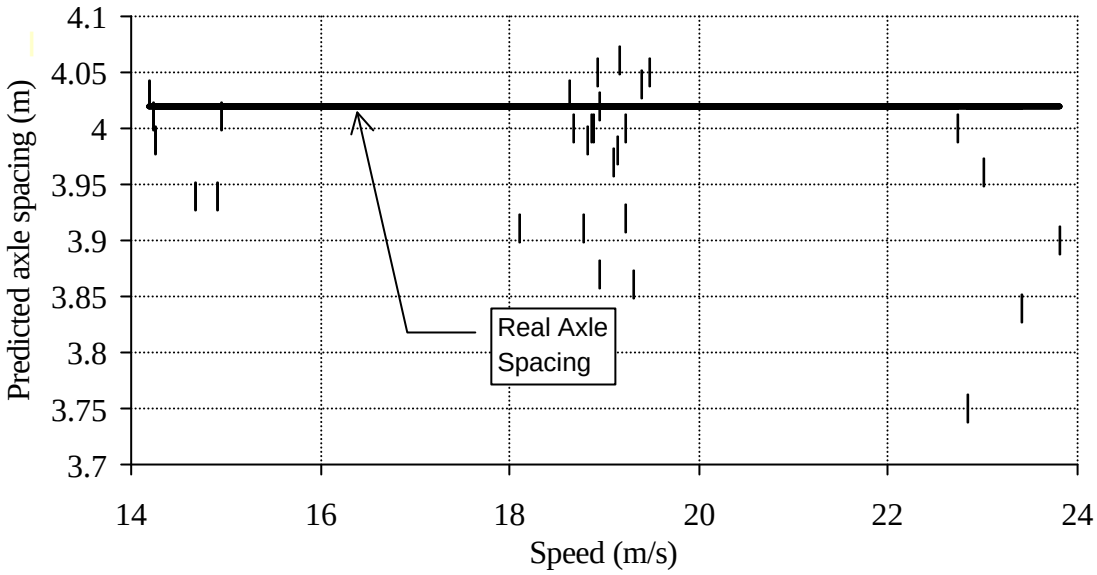

Figure 4.29 – Predicted axle spacing at different speeds for a real axle spacing of 4.02 m

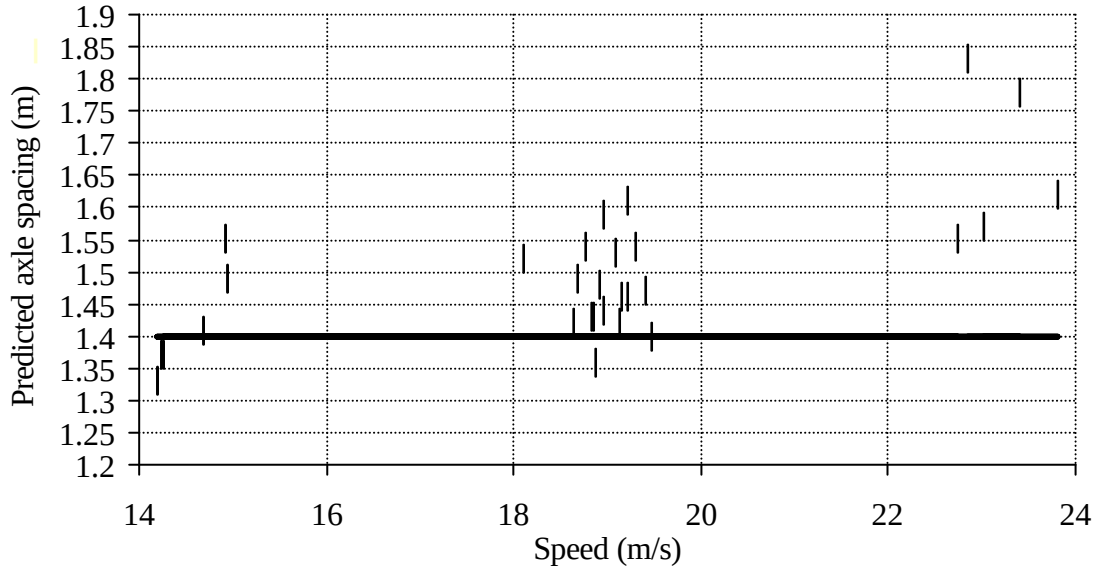

Figure 4.30 – Predicted axle spacing at different speeds for a real axle spacing of 1.40 m

In practise, there are sources of inaccuracy other than scanning frequency. For example, transverse location of the truck may cause errors and there are cases where directions of traffic flow are not perpendicular to the tube. As experienced in Delgany site, very closely spaced axles can induce two pulses of air, one immediately behind the other, distorting a clear record. An excessive length or twisting of the tube can also cause problems. Hence, the average measured errors from the figures above have been – 6 cms for the spacing between 1st and 2nd axle (spaced at 4.02 m), 9 cms for the 2nd and 3rd axle (spaced at 1.40 m), and 3 cms for the 1st and 3rd axle (spaced at 5.42 m). Best results are achieved for the

whole vehicle length. The accuracy of the latter improves the synchronisation between strains and truck location along the bridge.

Objectives of the Program

Initially, there was a Turbo-C program developed by Dempsey (1997) based on Moses' algorithm and a theoretical longitudinal beam model that analysed the signal corresponding to an isolated traffic event. The program also indexed the strain record by giving the starting and ending points for each truck crossing event to a binary file with the whole strain record. This binary file was acquired with DAQ software based in C and developed by O'Connor (1994). These pointer numbers depended on the signal given by the axle detectors, and so, when axle detectors failed to identify the vehicle, part of the strain record could have been missing and its recovery could be a tedious (if not, impossible) task. Therefore, the author re-wrote the code in C++ to allow:

- Reading an experimental influence line as a function of distance from a text file.
- Reading any input (binary or text) strain record.
- Introducing an interface to modify parameters readily, such as calibration factors, bridge length and truck characteristics (initially, the code had to change some values and be re-compiled every time one of these factors was varied).

The author, McNulty (1999) and Kessler (1997) used this new version for analysing the impact of an improved influence line on B-WIM accuracy (Section 3.7.4).

The Irish B-WIM program was originally designed to deal with one single vehicle at a time where strain record, number of axles, axle spacings and velocity had to be input manually. It was necessary to automate the processing of vast amounts of voltage data and a lot of traffic information continuously. It was the author's task to process the recorded voltage data from axle detectors and strain sensors into number of axles, speeds, axle spacings and axle weights. This task was accomplished by implementing the post-processing axle detection algorithm and Moses' algorithm described previously. As a result, traffic data corresponding to thousands of vehicles for two uninterrupted weeks was obtained to calibrate the Eurocode Bridge model for Irish conditions (O'Brien et al. 1998b). The findings of this test will be discussed in Chapter 8. This software was developed in a DOS platform and it is included in the CD-ROM attached in this thesis.

General Structure of the Irish B-WIM Program

The program was originally written in Turbo C++ v.3.0, while last modifications have been made in Borland C++ 4.5. Given the large quantity of data being recorded, the first stage of the process was the removal of redundant data to minimise storage. Every 280 minutes and 12 channels take 184.8 MB of hard disk space (950.4 MB/day). Accordingly, from the total information on voltage, great savings can be made if only times and strains when there is traffic on the bridge are stored. First of all, binary Labview is converted into text. This text file is between four and five times greater than the original Labview file. Then, the text file is reconverted into binary C (data format: floating point 16 bits) to save space in hard disk and facilitate further post-processing. Then, data is converted into axle hits first, velocity and axle spacings in a second stage and finally into weights. The flow and intermediate processes of the program are summarised in Figure 4.31.

The main menu of the B-WIM program displays the following options:

A. Data acquisition
B. Voltage signal
C. Strain & time storage
D. Calibration
E. Calculation of Weights
F. Files
Q. Quit

The access to the different options is organised through **.bat* files. Option A links the B-WIM interface with DAQ software and applications. Option B is related to signal analysis and a consideration of the most convenient choice of parameters for axle detection or the strain definition at different locations. Option C saves the parts of the voltage file corresponding to when there is traffic on the bridge. Option D provides a facility to look for a test vehicle in a file and determines the calibration factor as defined in Equation 2.1. Option E calculates weight data for a given voltage file. Option F displays the available files (i.e. voltage, strains, times, WIM data, information/model, header and source files). Further details on the contents of the program are given in Appendix D.

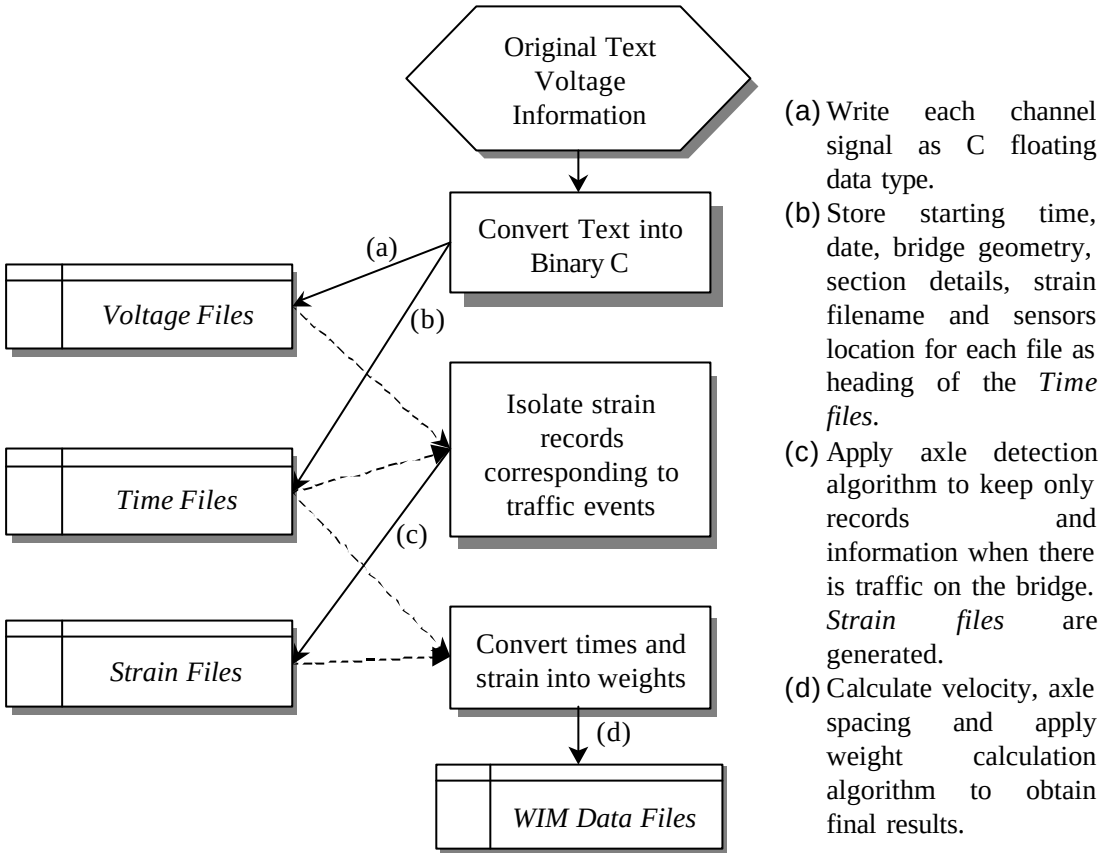

Figure 4.31 – General structure of the program

4.5 Summary

B-WIM systems estimate traffic loads from the bending that vehicles cause as they cross a bridge. This chapter has described the two types of device used by the Irish team to measure bending: (a) strain gauges, generally used in flexible bridges (i.e., steel bridges such as Belleville -Section 8.4.1-), and (b) mechanical strain amplifiers, used in stiff bridges, where a better strain definition is necessary. These amplifiers are bolted to the bridge and they are made of strain gauges connected in a quarter or full Wheatstone configuration. There is also a need to detect axles, which can be done in two different ways:

- From sensors mounted in/on the road surface, e.g., tape switches, rubber tubes, piezo electric sensors. Piezo electric sensors are expensive and extreme care must be taken during installation to ensure good results. Tape switches are very sensitive to traffic aggressiveness. The Irish team has obtained best results with rubber tubes, though they

can only be used in conditions of low traffic intensity and their attachment to the road must be checked periodically.

- From strain sensors attached to the soffit of the bridge (FAD). FAD systems are a very promising technology currently under development. One of their main limitations has been the reduced number of sites where they can be implemented successfully (i.e., orthotropic decks and short span slab bridges). First theoretical studies indicate that integral bridges with spans shorter than 10 m might qualify for FAD purposes.

Concerning the data acquisition hardware, the Irish B-WIM system has used National Instruments equipment that allows for scanning at rates of up to 333 kS/s. The increase in scanning frequency and number of channels that can be recorded simultaneously has made possible the development of FAD systems and multiple-sensor algorithms. Hardware low pass filters make the original data unrecoverable and they should not be applied unless there is certainty that no significant component of the signal is removed. The use of a 16-bit DAQ card instead of a 12-bit card improved resolution significantly.

All the information provided by strain sensors and axle detectors was recorded in a computer through data acquisition software. Originally, the information is recorded in binary format to save storage space and time. This system can be managed manually or left unattended on site for long periods of time. During post-processing, raw data from the different channels is converted into vehicle classification, weights, speeds, headways and gaps. A program to automate this process for two lanes of traffic has been developed by the author. The code implements two algorithms:

- An axle detection algorithm to convert signal from road sensors into number of axles, axle spacings and speed. There are also several routines that detect and deal with outliers and/or doubtful values (i.e., undetected axles by axle detectors or changes of lane).
- An algorithm for weight calculation based on static equations. This algorithm has been described in Section 3.3.

The program has been used to process data uninterruptedly from an Irish site and obtain traffic statistics necessary for the calibration of the bridge load model for Irish conditions (Section 8.2.3).